NANO LETTERS

2007
Vol. 7, No. 10
3235−3240

A Molecular Spectroscopic Description of Optical Spectra of J-Aggregated Dyes on Gold Nanoparticles

Anne Myers Kelley[†]

School of Natural Sciences, University of California, P.O. Box 2039, Merced, California 95344

Received August 15, 2007

ABSTRACT

The extinction spectra of J-aggregated dyes on gold nanoparticles, which exhibit interferences between the plasmonic and dye resonances, are simulated by a quantum mechanical model that considers the dye transition to interact through transition-dipole coupling with a continuum of nanoparticle states. This alternative to the classical core–shell dielectric model provides the wavefunctions of the coupled molecule–nanoparticle system and qualitatively explains the enhancement of resonance Raman, fluorescence, and other light-driven processes of molecules adsorbed to nanoparticles.

Several recent papers have reported the optical extinction spectra (absorption plus scattering) of strongly absorbing, J-aggregated organic dyes adsorbed to gold or silver nanoparticles or surface nanostructures.[1−5] These spectra are not simple superpositions of the surface plasmon spectra of the metal and the absorption spectra of the dyes nor do they exhibit obviously increased dye absorbance as a straightforward interpretation of the electromagnetic field enhancement mechanism for surface-enhanced spectroscopies might suggest.[6] Rather, the optical spectra of these dye/nanoparticle composites exhibit what appear to be interferences between the molecular and plasmon resonances. Typically these spectra have been explained by treating the dye/nanoparticle system as a particle consisting of a core and a shell having different dielectric functions. Classical electrodynamics[7] can then be used to calculate the optical properties, analytically for spherical particles and numerically for arbitrary shapes. When realistic dielectric functions for the bulk metal and the dye are used, this approach generates optical spectra quite similar to those observed experimentally. The interferences are attributed to the variation in phase of the optical polarization induced by excitation on the red and blue sides, respectively, of any resonance.

While classical electrodynamics can successfully describe the extinction spectra of dye/nanoparticle composites, its limitations become evident when other experimental observables are considered. One such observable is surface-enhanced (resonance) Raman scattering (SE(R)RS). Resonance Raman intensities depend on the details of the excited-state vibronic wavefunctions and their line widths.[8−11] SERS away from molecular electronic resonance is typically attributed to the enhancement of the incident and scattered electric fields caused by coupling with the surface plasmons of the metal. However, classical descriptions that provide only the frequency-dependent polarizability of the core−shell particle do not capture the quantum-mechanical details of the hybrid wavefunctions needed to calculate resonance Raman intensities.[12−14] Therefore we have sought a quantum mechanical approach to describe these systems. Coupling between a discrete transition of a bound chromophore or dye aggregate to the plasmon resonance of a metal can be considered an example of the more general coupling of a discrete state to a continuum as developed by Fano[15] and widely applied in molecular spectroscopy. This view was also taken by Lee and Birman in their discussion of SERS.[16] Here we develop the details of this approach and use it to describe the optical spectra of J-aggregate/nanoparticle composites. Other workers have recognized the utility of a quantum-mechanical model for describing dye/nanoparticle spectra and have discussed qualitative quantum-mechanical models[3] but have not shown spectral simulations using such models.

Consider that the plasmon excitations of the metal nanoparticle give rise to a large, isotropic transition dipole moment. The width of the plasmon resonance arises from a variety of factors as discussed further below; here we model it as a continuous distribution of excitations having well-defined energies. Although a finite-sized nanoparticle has a finite number of excitations, in practice they are sufficiently close together to be considered continuous. The coupling mechanism is taken here to be the dipole−dipole interaction

[†] E-mail: amkelley@ucmerced.edu.

10.1021/nl072054d CCC: $37.00
Published on Web 09/11/2007

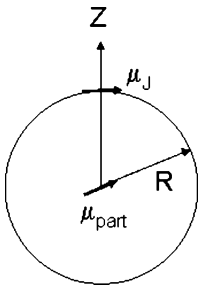

Figure 1. Geometry of the J-aggregate/nanoparticle composite.

between the transition dipole of the molecule and the continuum of transition dipoles of the particle. Dipole−dipole coupling is clearly inadequate when the dye is sitting on or very near the surface of the nanoparticle, but it presents a simple starting point. The J-aggregated dye is assumed to sit on the surface of a spherical nanoparticle of radius R, with its transition dipole $\vec{\mu}_J$ tangent to the surface of the sphere (perpendicular to $\vec{R}$) as shown in Figure 1. The z-axis of the system is defined by the line connecting the center of the particle to the center of the J-aggregate, and $\vec{\mu}_J$ is defined to lie along the x-axis. As a spherical particle is an isotropic oscillator, the polarization direction of the incident light defines the direction of the nanoparticle's transition dipole, $\vec{\mu}_{part}$, which is randomly distributed in θ and φ.

The dipole−dipole interaction energy[17] for this geometry is $U_{\mu\mu} = \mu_1\mu_2/R^3 \sin\theta \cos\varphi$; in units of cm^{-1}, this is

$$U_{\mu\mu} = 1.159 \times 10^5 \frac{r_J r_{part}}{R^3} \sin\theta \cos\varphi \tag{1}$$

where the transition lengths r and particle radius R are both in angstroms.

We seek the wavefunctions and energies for the new states that result from coupling the molecular state to the nanoparticle states through this dipole−dipole interaction. This is the general problem solved by Fano,[15] but his development, in its simplest form, describes the coupling of a delta-function discrete resonance to a continuum. The strongly allowed, lowest-lying excitonic transition of a molecular J-aggregate in the absence of the metal is narrow by the standards of condensed-phase organic molecular spectroscopy but it is far from a delta function; at ambient temperatures it is typically broadened to a few hundred cm^{-1} by some combination of inhomogeneous broadening, radiative and nonradiative decay, and coupling to low-frequency vibrations. Thus we need to invoke Fano's situation of "one discrete state and two or more continua". We label the discrete state of the J-aggregate as φ_J, the continuous states of the nanoparticle as $\phi_{part}(E)$, and the continuous states of the other (henceforth referred to as "solvent") continuum as $\chi_{solv}(E)$. We assume that the Hamiltonian involving the continuum states alone has already been diagonalized and make the further assumption that the coupling matrix element between the J-aggregate and the solvent is independent of energy. The off-diagonal matrix elements of the total system Hamiltonian thus take the form

$$\langle\varphi_J|H|\varphi_{part}(E)\rangle = V(E,\theta,\varphi) \tag{2a}$$

$$\langle\varphi_J|H|\chi_{solv}(E)\rangle = W \tag{2b}$$

$$\langle\chi_{solv}(E')|H|\varphi_{part}(E)\rangle = 0 \tag{2c}$$

where we explicitly indicate the dependence of the dipole−dipole interaction energy on both the energy of the nanoparticle state and the angle between the two transition moments. Diagonalization of this Hamiltonian leads to two solutions at each energy[15]

$$\psi(E,\theta,\varphi) = a(E,\theta,\varphi)\varphi_J + \int dE'[b(E,E',\theta,\varphi)\phi_{part}(E') + c(E,E',\theta,\varphi)\chi_{solv}(E')] \tag{3a}$$

$$\psi'(E,\theta,\varphi) = \int dE'[b'(E,E',\theta,\varphi)\phi_{part}(E') + c'(E,E',\theta,\varphi)\chi_{solv}(E')] \tag{3b}$$

The coefficients of interest are given by

$$a(E,\theta,\varphi) = \frac{\sin\bar{\Delta}_{E,\theta,\varphi}}{\pi[V^2(E,\theta,\varphi) + W^2]^{1/2}} \tag{4a}$$

$$b(E,E',\theta,\varphi) = \frac{V(E',\theta,\varphi)}{[V^2(E,\theta,\varphi) + W^2]^{1/2}}\left[\frac{1}{\pi}\frac{\sin\bar{\Delta}_{E,\theta,\varphi}}{E - E'} - \cos\bar{\Delta}_{E,\theta,\varphi}\delta(E - E')\right] \tag{4b}$$

$$b'(E,E',\theta,\varphi) = \frac{W\delta(E - E')}{[V^2(E,\theta,\varphi) + W^2]^{1/2}} \tag{4c}$$

with

$$\bar{\Delta}_{E,\theta,\varphi} = -\arctan\frac{\pi[V^2(E,\theta,\varphi) + W^2]}{E - E_J - G(E,\theta,\varphi)} \tag{5a}$$

$$G(E,\theta,\varphi) = P\int dE'\frac{V^2(E,\theta,\varphi) + W^2}{E - E'} \tag{5b}$$

The states of the "solvent" continuum are assumed to be completely nonresonant in the region of interest and do not contribute to the optical spectrum. Therefore the absorption spectrum at energy E is proportional to

$$\sigma(E,\theta,\varphi) \propto E\{|a(E,\theta,\varphi)\vec{r}_J\cdot\hat{z} + \int dE'b(E,E',\theta,\varphi)r_{part}(E')|^2 + |\int dE'b'(E,E',\theta,\varphi)r_{part}(E')|^2\} \tag{6}$$

where $\vec{r}_J$ is the transition dipole length of the J-aggregate and $r_{part}(E)$ is the transition dipole length of the nanoparticle at energy E.

$V(E,\theta,\varphi)$ is the coupling matrix element between the molecular state and the nanoparticle state having energy E. Note that V^2 and W^2 must have units of energy, not energy

squared—these quantities are in energy squared per unit energy increment. V can be obtained from the transition dipole moment of the nanoparticle at energy E, which in turn is calculated from the nanoparticle's absorption spectrum. If we consider the optical absorption spectrum to be composed of a continuous distribution of delta functions, the relationship between the optical absorption cross section at energy E and the transition dipole length at that energy is given by[11]

$$r(E) = \left[\frac{\sigma(E)}{E}\frac{3\hbar c}{4\pi^2 e^2}\right]^{1/2} \tag{7}$$

The conversion from extinction coefficient in M^{-1} cm^{-1} (ϵ) to cross section in $Å^2$ (σ) is given by $\sigma = (2.303 \times 10^{19})\epsilon/N_A = (3.83 \times 10^{-5})\epsilon$. For 10 nm diameter gold particles, which have a molar extinction coefficient of 6.15×10^7 M^{-1} cm^{-1} at 450 nm,[18] the maximum absorption cross section (at 520 nm) is 4044 $Å^2$.

The final step is to average the absorption spectrum over a random distribution of angles

$$\sigma(E) \propto \int_0^{2\pi} d\varphi \int_0^{\pi} \sin\theta \, d\theta \sigma(E,\theta,\varphi) \tag{8}$$

Taking an incoherent average over angles amounts to assuming that the coherence length of a single J-aggregate is much smaller than the size of the nanoparticle.

Calculations of representative spectra were carried out using the following parameters. The Au nanoparticles were assumed to be spherical with a 10 nm diameter as in refs 4 and 5; similar effects have been observed in much larger[2] and/or nonspherical[3] particles. To obtain the Au nanoparticle spectrum, we measured the optical extinction spectrum (which is almost entirely absorption, rather than scattering, for small particles)[7] of ~10 nm aqueous colloidal gold nanoparticles prepared in our laboratory through the standard citrate reduction method.[19] The measured spectra were scaled to the molar absorptivity of gold nanoparticles of this size according to Haiss et al.[18] For the dye, we assumed a single-molecule transition dipole length of 2 Å. Estimated coherence lengths for J-aggregated cyanine dyes vary from a few to nearly 100 depending on temperature, environment, molecular structure, and method of measurement.[20−24] We assumed an arbitrary but reasonable coherence length of eight monomer units at room temperature, giving an effective transition dipole length of 5.7 Å for the J-aggregate. The dye/solvent coupling parameter, W, was chosen to give a Lorentzian line width, in the absence of nanoparticles, of about 380 cm^{-1}.[2,4] The resonance frequency of the dye absorption was varied in order to probe the dependence of the coupled absorption spectrum and eigenstates on the relative energies of the J-aggregate and plasmon resonances.

Figure 2 demonstrates how varying the strength of the dye−metal coupling affects the optical spectrum. When the J-aggregate and the nanoparticle are weakly coupled by assuming a center-to-center distance of 50 nm, much greater than the size of the particle, the spectrum of dye plus Au is nearly indistinguishable from that of the Au nanoparticle alone. However, when the distance is reduced to 5 nm (the physical radius of the particle), interference between the two resonances results in a strong "dip" in the plasmon spectrum at the dye resonance frequency. The change in absorbance at the dye frequency is much larger than the absorbance of the dye alone; the two resonances interfere destructively, and the effect of the dye is magnified by its coupling with the much stronger nanoparticle absorbance. Note, however, that this model does conserve the total oscillator strength, with the dip at the dye resonance being compensated by a slightly increased absorbance at higher energies.

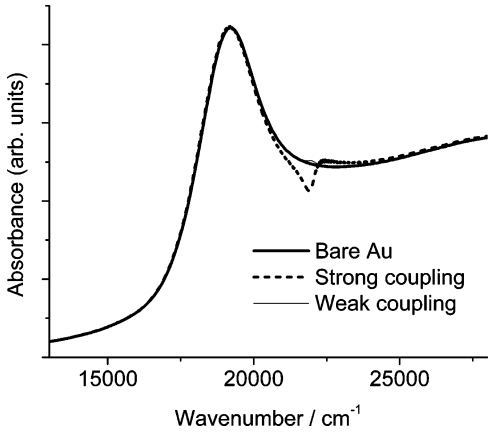

Figure 2. Calculated absorbance spectrum of J-aggregated dye on 10 nm diameter Au nanoparticles ($E_J = 22000$ cm^{-1}, $r_J = 5.7$ Å, $W^2 = 56$ cm^{-1}). The "strong coupling" and "weak coupling" spectra are generated by assuming dye−particle distances of 5 and 50 nm, respectively. The "weak coupling" spectrum is almost indistinguishable from the bare Au spectrum.

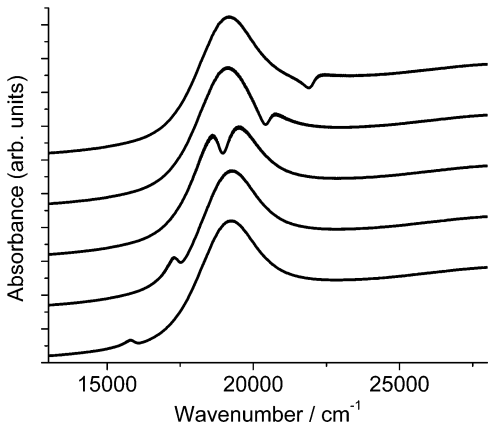

Figure 3. Calculated absorbance spectra of J-aggregated dye on 10 nm diameter Au nanoparticles ($r_J = 5.7$ Å, $W^2 = 56$ cm^{-1}, $R =$ 5 nm). The dye resonance energies E_J are (bottom to top) 16000, 17500, 19000, 20500, and 22000 cm^{-1}.

Figure 3 demonstrates the effect of tuning the molecular resonance frequency in the strong coupling case. As previous experimental studies have shown,[4,5] when the molecular-resonance lies to the red of the plasmon resonance the two transitions interfere largely constructively to give increased absorbance at the dye resonance frequency, while destructive interference is observed on the blue side.

The calculated spectra in Figures 2 and 3 are qualitatively similar to those generated from purely classical, core−shell

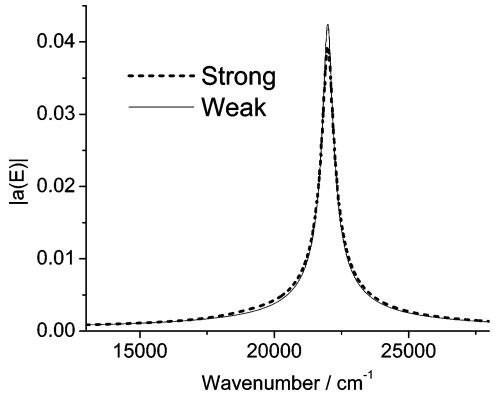

Figure 4. Angle-averaged absolute value of coefficient of J-aggregate wavefunction in the eigenstates ($E_J = 22000$ cm^{-1}, $r_J = 5.7$ Å, $W^2 = 56$ cm^{-1}). The "strong coupling" and "weak coupling" spectra are generated by assuming dye−particle distances of 5 and 50 nm, respectively, as in Figure 2.

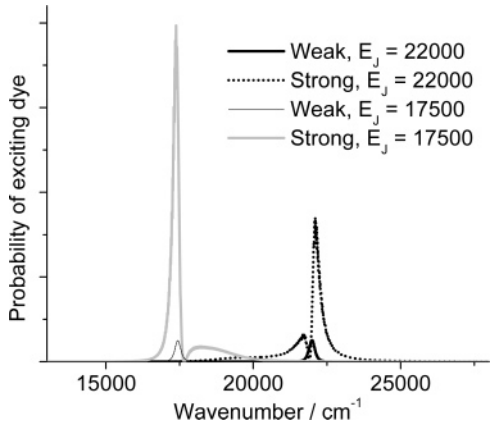

Figure 5. Relative probability of exciting the J-aggregate state for the cases of strong coupling ($R = 5$ nm) and weak coupling ($R = 50$ nm) as calculated from eq 12. In each case $r_J = 5.7$ Å and $W^2 = 56$ cm^{-1}. Results are shown for dye energies on both the red side and the blue side of the plasmon band. Figures 2 and 3 show corresponding total absorbance spectra.

dielectric models.[2−5,25] The advantage of a quantum-mechanical model is that it provides the wavefunctions contributing to the absorbance at each energy. The angle-averaged contribution of the J-aggregate wavefunction to the composite wavefunction at energy E is given by $\int d\varphi \int \sin\theta\, d\theta |\langle\varphi_J|\psi(E,\theta,\varphi)\rangle| = \int d\varphi \int \sin\theta\, d\theta |a(E,\theta,\varphi)|$. This quantity is plotted for the cases of both strong and weak coupling in Figure 4. Surprisingly, the distribution of the dye wavefunction into the coupled eigenstates does not differ much between the strong coupling and weak coupling regimes, even though these two cases lead to very different absorption spectra as shown in Figure 2. The differences are similarly small when the coefficients are examined at each individual angle or when the coefficient itself rather than its modulus is plotted.

The results of Figure 4 might suggest that observables that depend upon direct excitation of the dye should not be greatly perturbed by the presence of the metal. That this is not correct can be demonstrated using time-dependent perturbation theory. Before the light is turned on at $t = 0$, the system is in state ψ_g, where both molecule and nanoparticle are in their electronic ground states. After a weak perturbation at frequency $\omega = E/\hbar$ is turned on, the state of the system is, in general, a superposition of all of its eigenstates

$$\Psi(E,\theta,\varphi,t) = \psi_g + \int dE' \alpha_{E,E',\theta,\varphi}(t)\psi(E',\theta,\varphi) + \int dE' \alpha'_{E,E',\theta,\varphi}(t)\psi'(E',\theta,\varphi) \quad (9)$$

where the states $\psi(E',\theta,\varphi)$ and $\psi'(E',\theta,\varphi)$ are given in eqs 3. The coefficients α are found from the usual formulas of first-order time-dependent perturbation theory with a very weak, monochromatic field in the long-time limit as

$$\alpha_{E,E',\theta,\varphi}(t) = 2\pi t \frac{\langle\psi(E',\theta,\varphi)|\vec{\mu}\cdot\hat{z}|\psi_g\rangle}{\hbar} \times \exp(-iE't/\hbar)\delta(E'/\hbar - \omega) \quad (10)$$

and analogously for α'. In the long-time limit the perturbed part of the wavefunction is

$$\Psi^{(1)}(E,\theta,\varphi,t) \propto \langle\psi(E,\theta,\varphi)|\vec{\mu}\cdot\hat{z}|\psi_g\rangle \exp(-iEt/\hbar)\psi(E,\theta,\varphi) + \langle\psi'(E,\theta,\varphi)|\vec{\mu}\cdot\hat{z}|\psi_g\rangle \exp(-iEt/\hbar)\psi'(E,\theta) \quad (11)$$

The angle-averaged probability of finding the system in the J-aggregate excited state when excited at energy E is given by $P_J(E) = \int d\varphi \int \sin\theta\, d\theta |\langle\varphi_J|\Psi^{(1)}(E,\theta,\varphi,t)\rangle|^2$. Substituting eqs 3 into eq 11 gives

$$P_J(E) \propto \int d\varphi \int \sin\theta\, d\theta \{|a(E,\theta,\varphi)|^2 |a(E,\theta,\varphi)(\vec{\mu}_J\cdot\hat{z}) + \int dE' b(E,E',\theta,\varphi)\mu_{part}|^2\} \quad (12)$$

This quantity is plotted in Figure 5 for the cases of both strong and weak coupling and for two different choices of the J-aggregate resonance energy E_J. In the weak coupling limit, the total absorbance spectrum is essentially the sum of the separate dye and nanoparticle absorbances (Figure 2) and the probability of exciting the dye is a Lorentzian centered at the dye resonance frequency and having the isolated dye's line width. When the coupling is strong, the spectrally integrated probability for exciting the dye becomes much higher and varies sharply with wavelength, and significant excitation of the dye can occur at frequencies that lie well outside the absorption band of the isolated dye.

The classical picture of the plasmon absorption is that it consists of a single, collective oscillation of the conduction electrons which is strongly damped to produce the observed plasmon widths of ~2000 cm^{-1}. A variety of experimental measurements have been interpreted to show "T_2" or "dephasing" times of 10 fs or less.[26] These results seem at odds with our description of the plasmon absorption band as a quasi-continuum of individually sharp transitions whose spectral density reproduces the experimental extinction spectrum. However, terminology with respect to dephasing is often ill-defined; for example, the dephasing time for an electronic transition of a large dye molecule in solution is often stated to be the inverse of a single molecule's

absorption bandwidth, even though most of this width is a manifestation of spectral congestion (vibronic structure and excitation of solvent nuclear motions). The visible absorption spectra of very small gold clusters clearly consist of a number of discrete transitions,[27] but the extent to which a spectral congestion model is applicable to the broad absorption bands of larger particles is less clear.[28,29] In order to address this question, we have also simulated the absorption spectra of the dye−nanoparticle composite using a density matrix approach that treats the nanoparticle and dye resonances each as single oscillators broadened by pure dephasing, plus an interaction term that allows for coherence transfer between the dye and the nanoparticle. This approach yields coupled absorption spectra that are essentially identical with those calculated from the Fano approach as long as the isolated dye and nanoparticle spectral densities used in the Fano method are chosen to give the same uncoupled spectra as in the density matrix approach. That is, for linear spectroscopic observables all that matters is the spectral density, not the details of how it arises.

The calculated spectra shown in Figures 2 and 3 capture the qualitative features of the experimental spectra of refs 4 and 5. No quantitative comparisons are attempted for several reasons. The assumption that the dye and the nanoparticle interact through simple transition dipole coupling is a major oversimplification as mentioned above. However, as long as the dye is merely physisorbed to the metal or chemisorbed through a linking group that is not directly involved in the electronic transition, orbital overlap between the molecule and the metal should be minimal and an empirical rescaling of the interaction matrix elements may be adequate. A more serious limitation is the assumption that only one J-aggregate interacts with each nanoparticle. In the systems that have been studied experimentally, it is believed that the surface of the metal is more or less completely covered with dye molecules and would best be described as a single nanoparticle interacting with tens to hundreds of individual J-aggregates. This is one reason why the experimental spectra[4,5] are more strongly perturbed, relative to the bare nanoparticle spectra, than the calculated spectra of Figure 3. The case of multiple discrete resonances interacting with a continuum is also addressed in Fano's paper,[15] but its extension to two continua, needed to account for the nonzero line width of the free J-aggregate, is more involved and will be deferred to a later paper.

Figure 2 shows that when the dye−metal coupling is strong, the optical spectrum is substantially different from the sum of the spectra of the individual components. Nevertheless, Figure 4 shows that the energy distribution of the components of the dye wavefunction, which is already mixed with the states of the "solvent" continuum to give its initial ~380 cm^{-1} Lorentzian line width, is only slightly modified by further coupling with the plasmon resonance of the metal. This is very different from the situation in strongly coupled molecular dimers or larger aggregates, where the monomer's wavefunction may appear distributed over aggregate states that span 1000 cm^{-1} or more.[30−34] In the dye−metal nanoparticle case, the relatively sharp J-aggregate transition is embedded in a quasi-continuum of nanoparticle states that extend to both higher and lower frequencies, resulting in little net frequency shift of the dye's wavefunction components. Yet even though the molecular wavefunction makes a very small contribution to the composite eigenstates at energies far from the molecular resonance frequency, Figure 5 shows that excitation at such frequencies can still have a high probability for exciting the molecule because the transition dipole of the metal is so huge.[12−14]

Metal surface enhancement of processes that involve resonant electronic excitation of a chromophore are important in a number of contexts. These include surface-enhanced resonance Raman scattering (SERRS),[13,14,35] fluorescence (SEF),[36−38] and fluorescence resonant energy transfer,[39,40] as well as enhancement of chromophore absorption in organic photovoltaics and photosynthetic systems.[41,42] Excitation spectra for SERRS and SEF often track the nanoparticle's absorption spectrum quite closely and are usually much broader than those shown in Figure 5. This probably reflects the fact that the electronic spectra of the bare chromophores typically have considerable vibronic structure (not necessarily resolved) and are much broader than J-aggregate spectra. Incorporation of a more general multistate model for the chromophore will be the subject of future work.

References

(1) Lim, I.-I. S.; Goroleski, F.; Mott, D.; Kariuki, N.; Ip, W.; Luo, J.; Zhong, C. J. *J. Phys. Chem. B* **2006**, *110*, 6673.
(2) Uwada, T.; Toyota, R.; Masuhara, H.; Asahi, T. *J. Phys. Chem. C* **2007**, *111*, 1549.
(3) Wurtz, G. A.; Evans, P. R.; Hendren, W.; Atkinson, R.; Dickson, W.; Pollard, R. J.; Harrison, W.; Bower, C.; Zayats, A. V. *Nano Lett.* **2007**, *7*, 1297.
(4) Wiederrecht, G. P.; Wurtz, G. A.; Hranisavljevic, J. *Nano Lett.* **2004**, *4*, 2121.
(5) Kometani, N.; Tsubonishi, M.; Fujita, T.; Asami, K.; Yonezawa, Y. *Langmuir* **2001**, *17*, 578.
(6) Franzen, S.; Folmer, J. C. W.; Glomm, W. R.; O'Neal, R. *J. Phys. Chem. A* **2002**, *106*, 6533.
(7) Bohren, C. F.; Huffman, D. R. *Absorption and scattering of light by small particles*; Wiley-VCH: Weinheim, Germany, 1983.
(8) Kelley, A. M. *J. Phys. Chem. A* **1999**, *103*, 6891.
(9) Myers, A. B. *Acc. Chem. Res.* **1997**, *30*, 519.
(10) Myers, A. B. In *Laser Techniques in Chemistry*; Myers, A. B., Rizzo, T. R., Eds.; Wiley: New York, 1995; p 325.
(11) Myers, A. B.; Mathies, R. A. In *Biological Applications of Raman Spectroscopy*; Spiro, T. G., Ed.; Wiley: New York, 1987; Vol. 2; p 1.
(12) Michaels, A. M.; Nirmal, M.; Brus, L. E. *J. Am. Chem. Soc.* **1999**, *121*, 9932.
(13) Michaels, A.; Jiang, J.; Brus, L. *J. Phys. Chem. B* **2000**, *104*, 11965.
(14) Jiang, J.; Bosnick, K.; Maillard, M.; Brus, L. *J. Phys. Chem. B* **2003**, *107*, 9964.
(15) Fano, U. *Phys. Rev.* **1961**, *124*, 1866.
(16) Lee, T.-K.; Birman, J. L. *Phys. Rev. B* **1980**, *22*, 5953.
(17) Stone, A. J. *The Theory of Intermolecular Forces*; Oxford University Press: New York, 1996.
(18) Haiss, W.; Thanh, N. T. K.; Aveyard, J.; Fernig, D. G. *Anal. Chem.* **2007**, *79*, 4215.
(19) Lee, P. C.; Meisel, D. *J. Phys. Chem.* **1982**, *86*, 3391.
(20) Scheblykin, I. G.; Bataiev, M. M.; Van der Auweraer, M.; Vitukhnovsky, A. G. *Chem. Phys. Lett.* **2000**, *316*, 37.
(21) Özçelik, S.; Özçelik, I.; Akins, D. L. *Appl. Phys. Lett.* **1998**, *73*, 1949.
(22) Scheblykin, I. G.; Sliusarenko, O. Y.; Lepnev, L. S.; Vitukhnovsky, A. G.; Van der Auweraer, M. *J. Phys. Chem. B* **2001**, *105*, 4636.
(23) Lampoura, S. S.; Spitz, C.; Dahne, S.; Knoester, J.; Duppen, K. *J. Phys. Chem. B* **2002**, *106*, 3103.

(24) Potma, E. O.; Wiersma, D. A. *J. Chem. Phys.* **1998**, *108*, 4895.
(25) Ambjornsson, T.; Mukhopadhyay, G.; Apell, S. P.; Kall, M. *Phys. Rev. B* **2006**, *73*, 085412.
(26) Link, S.; El-Sayed, M. A. *Annu. Rev. Phys. Chem.* **2003**, *54*, 331.
(27) Aikens, C. M.; Schatz, G. C. *J. Phys. Chem. A* **2006**, *110*, 13317.
(28) Brack, M. *Rev. Mod. Phys.* **1993**, *65*, 677.
(29) de Heer, W. A. *Rev. Mod. Phys.* **1993**, *65*, 611.
(30) Fulton, R. L.; Gouterman, M. *J. Chem. Phys.* **1964**, *41*, 2280.
(31) Czikklely, V.; Forsterling, H. D.; Kuhn, H. *Chem. Phys. Lett.* **1970**, *6*, 207.
(32) Fidder, H.; Terpstra, J.; Wiersma, D. A. *J. Chem. Phys.* **1991**, *94*, 6895.
(33) Spano, F. C. *J. Chem. Phys.* **2002**, *116*, 5877.
(34) Kelley, A. M. *J. Chem. Phys.* **2003**, *119*, 3320.
(35) Weitz, D. A.; Garoff, S.; Gersten, J. I.; Nitzan, A. *J. Chem. Phys.* **1983**, *78*, 5324.
(36) Chen, Y.; Munechika, K.; Ginger, D. S. *Nano Lett.* **2007**, *7*, 690.
(37) Neumann, T.; Johansson, M.-L.; Kambhampati, D.; Knoll, W. *Adv. Funct. Mater.* **2002**, *12*, 575.
(38) Tam, F.; Goodrich, G. P.; Johnson, B. R.; Halas, N. J. *Nano Lett.* **2007**, *7*, 496.
(39) Malicka, J.; Gryczynski, I.; Fang, J.; Kusba, J.; Lakowicz, J. R. *Anal. Biochem.* **2003**, *315*, 160.
(40) Zhang, J.; Fu, Y.; Lakowicz, J. R. *J. Phys. Chem. C* **2007**, *111*, 50.
(41) Govorov, A. O.; Carmeli, I. *Nano Lett.* **2007**, *7*, 620.
(42) Rand, B. P.; Peumans, P.; Forrest, S. R. *J. Appl. Phys.* **2004**, *96*, 7519.

NL072054D